Stabilizing Stick-Slip Friction

Rosario Capozza,[1] Shmuel M. Rubinstein,[2] Itay Barel,[1] Michael Urbakh,[1] and Jay Fineberg[3]
[1]School of Chemistry, Tel Aviv University, 69978 Tel Aviv, Israel
[2]Department of Physics, Harvard University, Cambridge, Massachusetts 02138, USA
[3]The Racah Institute of Physics, The Hebrew University of Jerusalem, Givat Ram, Jerusalem 91904, Israel
(Received 21 March 2011; published 6 July 2011)

Even the most regular stick-slip frictional sliding is always stochastic, with irregularity in both the intervals between slip events and the sizes of the associated stress drops. Applying small-amplitude oscillations to the shear force, we show, experimentally and theoretically, that the stick-slip periods synchronize. We further show that this phase locking is related to the inhibition of slow rupture modes which forces a transition to fast rupture, providing a possible mechanism for observed remote triggering of earthquakes. Such manipulation of collective modes may be generally relevant to extended nonlinear systems driven near to criticality.

DOI: 10.1103/PhysRevLett.107.024301 PACS numbers: 46.55.+d, 46.50.+a, 81.40.Pq, 91.30.Px

While the frictional motion of a single block is often considered to be wholly deterministic, close examination reveals surprising variability. Stick-slip friction is one example. Although models [1] predict well-defined stick-slip frequencies, intervals between successive stick-slip events have relatively broad distributions [2].

Consider two blocks, as in Fig. 1(a), that are pressed together with a normal force, F_N. When a shear force, F_S, is applied to the edge of one of the blocks, the onset of motion in this "simple" frictional system is surprisingly complex. The nonuniform stress profile produced by F_S excites a sequence of rupture fronts; successive failure of the discrete contact ensemble that forms the interface between the blocks. Initiating well before the onset of macroscopic motion, each rupture propagates from the loaded edge and arrests prior to traversing the entire interface [3–6]. Such avalanchelike collective motion occurs in many forced physical systems where numerous discrete degrees of freedom are spatially coupled [7], in the vicinity of a phase transition. In friction each contact is near its rupture threshold.

The onset of motion is mediated by three distinct types of collective modes: rapid subsonic and supersonic ruptures as well as "slow" rupture fronts [8,9], nearly 2 orders of magnitude slower. Once initiated, the rupture velocities are coupled to the local ratio of shear/normal stress at the interface [9].

Interfaces [9] are locally much stronger than previously thought, sustaining local stress ratios a few times larger than the static friction coefficient without succumbing to motion. On the other hand, earthquakes can be triggered by small perturbations generated by either tidal forcing or other very remote earthquakes [10]. These questions motivated studies of slip onset in rock samples separated by a granular layer, upon application of sinusoidal perturbations to F_S [2,11,12]. Extending previous work on the effects of oscillatory modulation of F_N on reducing dynamic friction [13], the results suggested nontrivial dependencies on the phase [11], amplitude and frequency of the perturbation [2,12].

In experiments and in a simple model, we show that the random intervals between stick-slip events can be stabilized by adding a low amplitude oscillatory component to F_S. Moreover, a well-defined phase relation exists between the forcing function and the frictional onset with the phase locking related to a forced transition between slow to fast rupture modes.

Our experiments [Fig. 1(a)] were performed in ambient (20%–40%) humidity on optically flat interfaces composed of two PMMA blocks, a slider and a base, that were roughened to about 1 μm rms. The slider had (x, y, z) dimensions of (150, 6, 70) mm in the sliding, transverse and normal loading directions, respectively. The base blocks had (x, y, z) dimensions of (230, 30, 30) mm. A constant and uniform normal force, $1000 < F_N < 5000$ N

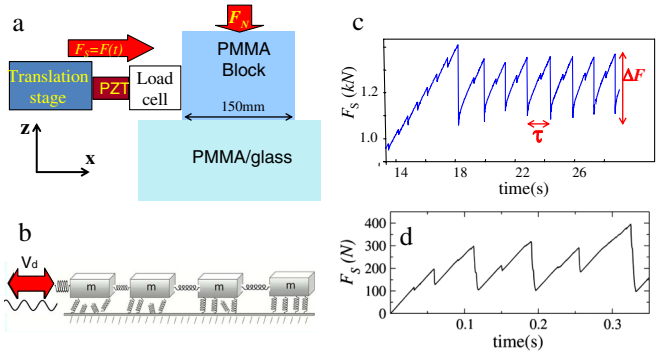

FIG. 1 (color online). Schematic views of the experimental system (a) and model (b). Typical stick-slip motion in experiments (c) and model (d) with no modulation of F_s. Parameter values used in the model: $F_N = 4000$ N, $K_d = 4 \times 10^7$ N/m, $M = 11.5$ kg, $V_0 = 10^{-4}$ m/s, $K = 10^8$ N/m, $\tau_r = 0.005$ s, $N_S = 20$, $N = 70$, $\gamma = 6462$ s^{-1}, $f_s = 1.37$ N, $\Delta f_s = 6.9 \times 10^{-3}$ N, $k = \langle k_i \rangle = 5 \times 10^6$ N/m, $\Delta = 1$ μm.

was imposed at the start of each experimental run. F_S was applied to the slider's trailing edge via a stiff load cell (Kister 9602A) in series with a piezoelectric actuator (Piezomechanik Gmbh) and a translational stage moving at constant velocity, V_0. A ramped and modulated loading force, $F_L = K_d[V_0 t + \Delta\cos(2\pi t/T)]$, was imposed, where $K_d \simeq 10^9$ N/m is the system stiffness, $0.001 < T < 3$ s and Δ are the oscillation period and amplitude. The real contact area, $A(x, t)$, was continuously measured, as in [8].

We model the experiments [Fig. 1(b)] by a slider of mass M interacting with an immobile rigid substrate. The slider is pushed from its trailing edge via a spring with a force $F_S = K_d[V_0 t + \Delta\cos(2\pi t/T) - X_t]$, where X_t is the position of the trailing edge. The slider is composed of N rigid blocks coupled by springs of rigidity, $K_{\rm int}$, so that $K_{\rm int} = (N-1)K$, where K is the slider rigidity. Friction is described in terms of interactions between each block and the substrate through an array of surface contacts. Each contact is modeled as a spring of elastic constant k_i connecting the block and the substrate, where $i = 1, 2, \ldots, N_s$, and N_s is the number of contacts. While a contact is intact, its spring elongates or shortens with the velocity of the corresponding block, producing a force $f_i = k_i l_i(t)$ inhibiting the motion, where $l_i(t)$ is the spring length. A contact breaks when f_i exceeds a threshold f_{si}. Contacts reattach in an unstressed state, after a delay time t_r taken from the distribution $P(t_r) = e^{-t_r/\tau_r}/\tau_r$, where τ_r is a characteristic time of contact formation. The thresholds f_{si} are chosen from a Gaussian distribution of mean f_s and standard deviation Δf_s. We consider f_{si} to be proportional to the area A_i of a given contact, while the transverse rigidity k_i is proportional to its size, $k_i \propto \sqrt{A_i}$. Therefore, the distributions of k_i and f_{si} are coupled by $k_i = k(f_{si}/f_s)^{1/2}$, where $k = \langle k_i \rangle$. When a contact reattaches, new values of f_{si} and k_i are assigned to it. Artificial vibrations of the blocks are avoided by introducing a viscous damping force, $f_\gamma = -m\gamma\dot{x}_j$, where x_j is the coordinate of the center of mass of the jth block of mass $m = M/N$.

Both the experiments and model are in the stick-slip regime of friction (Fig. 1). Under these loading conditions [3,6] large, system sized, stick-slip events are the culmination of a complex history of precursory rupture events that initiate at the system's trailing edge and arrest within the interface. The resulting slip generates discrete sequences of small sharp drops in $F_S(t)$ (Fig. 1) well below its peak values.

In the model, the shear stress accumulated at the trailing edge decays exponentially along the slider, with a corresponding deformation:

$$\Delta x_j = x_j - x_j^0 = \Delta x_1 \exp[-\sqrt{K_s/K_{\rm int}}(j-1)] \quad (1)$$

where x_j^0 is the equilibrium position of block j, Δx_1 is the displacement of the block at the trailing edge and $K_s = kN_S$. As F_S increases, the stress grows until it reaches the threshold for rupture of surface contacts at the first block. The experiments and simulations show that frictional sliding is stochastic in both the period between consecutive slip events (Fig. 2) and the size of the stress drops following each stick-slip event. The double peaked structure of the model's stick-slip interval distribution [Fig. 2(d)] reflects contributions of stick-slip events with different numbers of precursors.

What is the origin of the stochasticity of the frictional dynamics? The model has two sources of stochasticity: (i) a diversity of surface contacts characterized by distributions of rupture forces, stiffnesses and reattachment times, and (ii) nonlinearity of interactions between the driven spatially extended slider and the surface. Figure 2(d) demonstrates that a broad distribution of stick times is retained even when all contacts are *identical*. Thus, the stochastic response is mainly due to the nonlinearity. System nonlinearity leads to stochasticity only when the nonuniformly stressed region involves more than one block, i.e., $N \gg \sqrt{K_{\rm int}/K_s}$ [see Eq. (1)].

Once small harmonic perturbations are introduced to the shear loading, this picture changes significantly. Even relatively small perturbations can cause the interval, τ, between successive stick-slip events to phase lock to the perturbation frequency. This is clearly demonstrated in the histograms of τ for both experiments and simulations presented in Fig. 2. When a control signal is applied, the intervals between slip events are no longer randomly distributed around a mean value of τ_0. Instead, τ phase locks to the driving frequency, $2\pi/T$, attaining only integer values of T. The model also provides partial synchronization of stress drops, which is not clearly evident in the experiments. Phase locking occurs, in both experiments and model, not only for τ, but also for the intervals between successive precursors (see the supplemental material, Ref. [14]).

In the results presented in Fig. 2, T was the same order as τ. Phase locking also occurs for control frequencies that

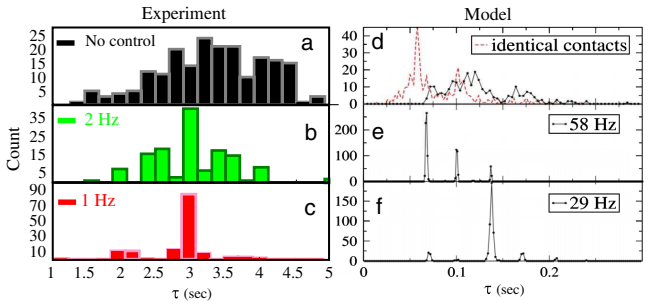

FIG. 2 (color online). Histograms of τ in experiments (left panels) and the model (right panels), when (a),(d) no external control is imposed, and for small-amplitude sinusoidal perturbations with external frequencies of 2 Hz (b), 1 Hz (c), 29 Hz (e), 58 Hz (f). The red dashed curve in (d) is a histogram calculated for identical surface contacts, when the system's nonlinearity is the only source of stochasticity. The model parameter values used are as in Fig. 1.

are much higher than the typical stick-slip frequency, τ_0. Figure 3 demonstrates that locking can occur at integer values n such that $\tau = nT$. The optimal modulation period, T, for synchronization of the stick-slip events is defined by the condition $nT = \tau_0$, where τ_0 is the mean stick-slip interval value in the absence of perturbations. This optimal period is given by Eq. (A2) in the supplemental material [14]. Once n is set, further increase (decrease) of T during a given experiment will "drag" τ to respectively higher (lower) values, within the initial distribution of stick-slip intervals.

Let us now define the phase, ϕ of stick-slip motion relative to the forcing by the temporal shift, Δt, from the peak of the force modulation, $\Delta\cos(2\pi t/T)$, that is closest to the slip event (see inset in Fig. 3). Thus, $\phi = 2\pi\Delta t/T$, and it lies in the interval $(-\pi, \pi)$. When the synchronization in Figs. 2 and 3 takes place, the system locks to a well-defined value of ϕ for each set of system parameters. A value $\phi = \phi_{\min}$ corresponding to a minimal possible value of the loading force, F_L, at the slip event is set by the condition that this force should be higher than the preceding maximum in the loading curve. This yields:

$$\phi_{\min} + \eta\cos(\phi_{\min}) \geq \Phi_{\max} + \eta\cos(\Phi_{\max}) \qquad (2)$$

where $\eta = (2\pi\Delta)/(TV_0)$ is a dimensionless parameter representing the ratio between the external harmonic control and the uniform background loading rate, and $\Phi_{\max}$ is the phase corresponding to the maximum loading force that is defined by $\sin(\Phi_{\max}) = 1/\eta$. For values $\eta < 1$, the loading force changes monotonically with time and harmonic oscillations do not influence the stick-slip pattern. For $\eta \gg 1$ Eq. (2) predicts asymptotic behavior, $\phi_{\min} \approx -2(\pi/\eta)^{1/2}$. These predictions are verified by both the experiments and simulations presented in Figs. 3(d) and 3(e): (i) η is indeed a relevant parameter that controls the frictional response to harmonic perturbations; (ii) A minimum value of $\eta \simeq 1$ exists, below which no phase locking is observed; (iii) When control is applied a well-defined "backbone" exists, below which the onset of stick-slip motion will (nearly) never occur; (iv) This backbone is described by: $\phi \propto -\eta^{-1/2}$. The data for stick-slip events are strongly clustered above this curve. The phases of the vast majority of the non-phase-locked data are, however, above the backbone. This may imply that a weaker sort of stochastic phase locking still persists. The $\phi \propto -\eta^{-1/2}$ scaling is, however, wholly consistent with previous measurements [11] in a granular system where strong phase locking was observed.

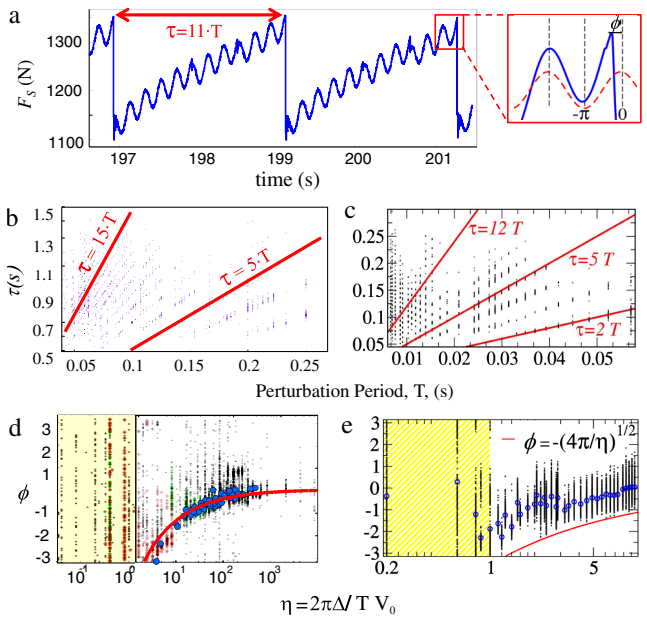

FIG. 3 (color online). Once phase locking occurs, τ becomes an integer multiple, n, of the forcing period, T. (a) A typical experiment for large n and $T \ll \tau_0$ (τ_0 is the, unperturbed, mean stick-slip interval). Stick-slip intervals, τ, as a function of T for experiments (b) and the model (c) over a broad range of loading conditions. The data all fall on well-defined lines of $\tau = nT$ for different integer values of n. Examples are highlighted by solid lines. Plots of ϕ vs η for experiments (d) and the model (e). Experiments: $1 < V_0 < 200$ μm/s, $2 < \Delta < 100$ μm, $0.1 < 2\pi/T < 500$ Hz. Phase locking is seen by the data clustering above a well-defined "backbone." At low values of $\eta = (2\pi\Delta)/(TV_0)$ (shaded region), no phase locking occurs and $-\pi < \phi < \pi$ occur with equal probability. As η is increased, correlated events appear with the initial phase of $-\pi$ for small η and saturate to zero for $\eta \gg 1$. Red curves in (d) and (e) correspond to $\phi_{\min} \approx -2(\pi/\eta)^{1/2}$. Blue dots are averaged values of ϕ for given values of η.

To clarify the synchronization mechanism of stick-slip events, we compare in Figs. 4(b) and 4(d) 2D maps of the fraction of attached contacts in the slider as functions of x and t in both the absence and presence of harmonic perturbations. The simulations show that the main effect of the perturbations on the detachment dynamics is the elimination of slow fronts. This effect is also observed experimentally in the contact area measurements [Figs. 4(a) and 4(c)], by driving the system at sufficiently large frequencies to enable us to capture their effect on the front dynamics.

What is taking place? Slow fronts arise [9] when the ratio of shear/normal stress is, locally, close to a critical, threshold value. An approximate 20% increase in this

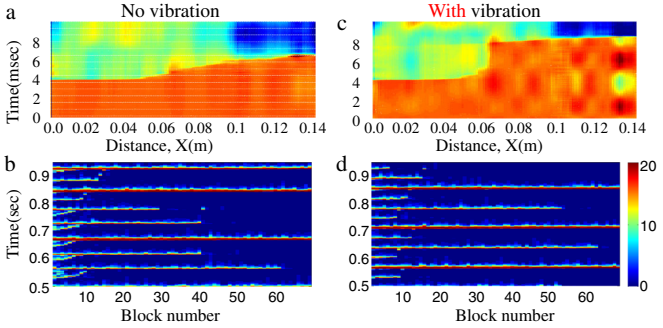

FIG. 4 (color online). Space-time maps of the measured real contact area (a),(c) and fraction of attached contacts in the model (b),(d) when no control is applied (left panels) and in the presence of oscillatory perturbations (right panels). Hotter (colder) colors indicate increased (decreased) contact area in (a),(c). (b),(d) The bars to the right of the maps set up a correspondence between the colors and the percent of detached contacts.

stress ratio is sufficient to trigger a transition to rapid rupture fronts. When applying stress to the system's trailing edge, its spatial distribution is highly nonuniform. Near the edge, as Eq. (1) indicates, the effect of the modulating component of F_S is therefore highly amplified and a 4%–5% overall modulation could easily be amplified to a 20% modulation near the edge. Thus, near the critical stress ratio, slow fronts are arrested/inhibited for $\phi < \phi_{\min}$ while rapid fronts may be triggered for $\phi > \phi_{\min}$. If the stress modulations are sufficiently rapid, slow fronts could not propagate long before rapid rupture is nucleated. We surmise that this is what is occurring in Fig. 4.

In summary, we have shown how small oscillatory perturbations can synchronize the periods between consecutive slip events. We identified one of the relevant dimensionless parameters and showed how it functionally affects the locking phase. We proposed a model, based on these results, that explains the experimental observations and elucidates the mechanism for phase locking. This picture may bear relevance to remote triggering of earthquakes. A fault which is susceptible to external triggering is most probably already close to criticality, perhaps approaching or within a state of slow, aseismic, rupture [15]. If the fault is subjected to nonuniform loading, a small amplitude, rapid stress oscillation radiated from a large faraway earthquake could be sufficient to trigger rapid, seismic, events, analogous to the one shown in Fig. 4.

Our results may have interesting ramifications beyond frictional systems. Our system is an example of a broad class of systems described by a large ensemble of nonlinearly coupled discrete variables that produce rich and complex collective behavior [7]. Thus, understanding how to excite and manipulate the collective modes involved in the stability of a simple rough frictional interface may provide insight into this general class of systems.

This work, as part of the ESF EUROCORES Program FANAS (ACOF), was supported by the Israel Science Foundation (1109/09). J. F. acknowledges support of the US-Israel Binational fund (Grant No. 2006288), the James S. McDonnell Fund and the European Research Council (Grant No. 267256). M. U. acknowledges support of the German-Israeli Project Cooperation Program (DIP).

[1] F. Heslot, T. Baumberger, B. Perrin, B. Caroli, and C. Caroli, Phys. Rev. E **49**, 4973 (1994); C. H. Scholz, Nature (London) **391**, 37 (1998).
[2] N. M. Beeler and D. A. Lockner, J. Geophys. Res. **108**, B82391 (2003).
[3] S. M. Rubinstein, G. Cohen, and J. Fineberg, Phys. Rev. Lett. **98**, 226103 (2007).
[4] O. M. Braun, I. Barel, and M. Urbakh, Phys. Rev. Lett. **103**, 194301 (2009).
[5] S. M. Rubinstein, I. Barel, Z. Reches, O. M. Braun, M. Urbakh, and J. Fineberg, Pure Appl. Geophys. (in press).
[6] S. Maegawa, A. Suzuki, and K. Nakano, Tribol. Lett. **38**, 313 (2010).
[7] K. A. Dahmen, Y. Ben-Zion, and J. T. Uhl, Phys. Rev. Lett. **102**, 175501 (2009); , Pure Appl. Geophys. (in press).
[8] S. Rubinstein, G. Cohen, and J. Fineberg, Nature (London) **430**, 1005 (2004); S. Nielsen, J. Taddeucci, and S. Vinciguerra, Geophys. J. Int. **180**, 697 (2010).
[9] O. Ben-David, G. Cohen, and J. Fineberg, Science **330**, 211 (2010).
[10] E. S. Cochran, J. E. Vidale, and S. Tanaka, Science **306**, 1164 (2004); J. Gomberg, P. Bodin, K. Larson, and H. Dragert, Nature (London) **427**, 621 (2004); A. L. Husker and E. E. Brodsky, Bull. Seismol. Soc. Am. **94**, S310 (2004); G. Hillers and Y. Ben-Zion, Geophys. J. Int. **184**, 860 (2011).
[11] H. M. Savage and C. Marone, J. Geophys. Res. **112**, B02301 (2007).
[12] P. A. Johnson, H. Savage, M. Knuth, J. Gomberg, and C. Marone, Nature (London) **451**, 57 (2008).
[13] M. Heuberger, C. Drummond, and J. N. Israelachvili, J. Phys. Chem. B **102**, 5038 (1998); M. G. Rozman, M. Urbakh, and J. Klafter, Phys. Rev. E **57**, 7340 (1998); A. Cochard, L. Bureau, and T. Baumberger, Trans. ASME **70**, 220 (2003); Z. Tshiprut, A. E. Filippov, and M. Urbakh, Phys. Rev. Lett. **95**, 016101 (2005); S. Jeon, T. Thundat, and Y. Braiman, Appl. Phys. Lett. **88**, 214102 (2006); A. Socoliuc *et al.*, Science **313**, 207 (2006); R. Capozza *et al.*, Phys. Rev. Lett. **103**, 085502 (2009).
[14] See supplemental material at http://link.aps.org/supplemental/10.1103/PhysRevLett.107.024301 for theoretical details.
[15] G. Rogers and H. Dragert, Science **300**, 1942 (2003); G. C. Beroza and S. Ide, Science **324**, 1025 (2009).